PHYSICAL REVIEW B VOLUME 26, NUMBER 6 15 SEPTEMBER 1982

Angle-resolved photoemission from polar and nonpolar zinc oxide surfaces

W. Göpel
Physics Department, Montana State University, Bozeman, Montana 59717

J. Pollmann
Institut für Physik, Universität Dortmund, Germany

I. Ivanov and B. Reihl
IBM Thomas J. Watson Research Center, Yorktown Heights, New York 10598
(Received 7 June 1982)

We report the first angle-resolved photoemission spectra (ARPES) of polar and nonpolar surfaces of an ionic wurtzite-type compound semiconductor. We present experimental results obtained at photon energies between 20 and 80 eV on the polar zinc and oxygen and the nonpolar $(10\bar{1}0)$ surfaces of ZnO and identify surface-induced features by comparison with recent theoretical calculations. Comparison between ARPES experiments and theory confirms the determination of the surface-atom geometry at ZnO$(10\bar{1}0)$ by low-energy electron diffraction studies.

I. INTRODUCTION

Angle-integrated and angle-resolved photoemission spectroscopy (AIPES and ARPES, respectively) are now widely accepted as powerful tools to investigate bulk and surface densities of electronic states. In contrast to a variety of studies on more covalent semiconductors like Si, Ge, or GaAs corresponding detailed investigations on highly ionic semiconductors including most of the II-VI compounds are missing. Besides a recent study on ZnSe(110),[1] few and only angle-integrated photoemission studies have been done so far on II-VI compounds.[2–11] In the present study we therefore investigated a typical II-VI compound semiconductor, i.e., ZnO, which exhibits polar [oxygen $(000\bar{1})$ and zinc (0001)] as well as nonpolar $(10\bar{1}0)$ cleavage faces (see Fig. 1). These different surfaces are expected to show pronounced differences in surface sensitive ARPES.

In earlier studies ZnO has served successfully as a model system to study ionic semiconductors: The nonpolar $(10\bar{1}0)$ surface in particular makes possible thermodynamically well-defined adsorption experiments[12,17] and its atomic geometry is well understood from low-energy electron diffraction (LEED) results and a dynamical LEED analysis.[12,13] Detailed theoretical calculations of electronic structures of all natural ZnO cleavage surfaces have been published recently[14] and will be used to compare the following experimental results with theory.

II. EXPERIMENTAL

Angle-integrated and angle-resolved photoemission spectra were measured with polarized light, a two-dimensional display-type spectrometer,[15] and a toroidal grating monochromator at the Synchrotron Radiation Center at Stoughton. An acceptance cone of 90° full angle around the sample normal was used for angle-integrated measurements

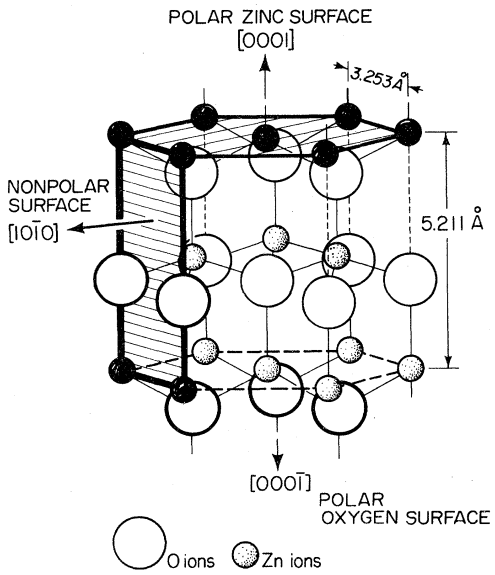

FIG. 1. Geometric structure of ZnO with the polar Zn(0001), O$(000\bar{1})$, and the nonpolar $(10\bar{1}0)$ cleavage surface.

 ©1982 The American Physical Society

while a single-channel detector accepting a cone of 8° full angle was used for angle-resolved measurements. The total energy resolution (electrons plus photons) was about 0.15 eV in the photon energy range 20—80 eV. For comparison, angle-integrated x-ray photoelectron spectra were taken in a conventional spectrometer with an Al $K\alpha$ source.

Zinc oxide surfaces were prepared by cleaving single crystals at 300 K under UHV. The samples were undoped and had a conductivity of $\sigma = 10^{-1}$ $(\Omega\,\mathrm{cm})^{-1}$ at 300 K. The working pressure in the UHV chamber was better than 10^{-8} Pa.

III. RESULTS AND DISCUSSION

Angle-integrated (AIPES) spectra will be discussed first in Sec. III A. The AIPES spectra have been obtained with an order of magnitude better signal-to-noise ratio than corresponding angle-resolved (ARPES) spectra and will serve to obtain an overview, to determine experimental conditions for high surface sensitivity, and to separate surface from bulk contributions to the photoemission process. We then discuss ARPES spectra in Sec. III B with particular emphasis on the determination of

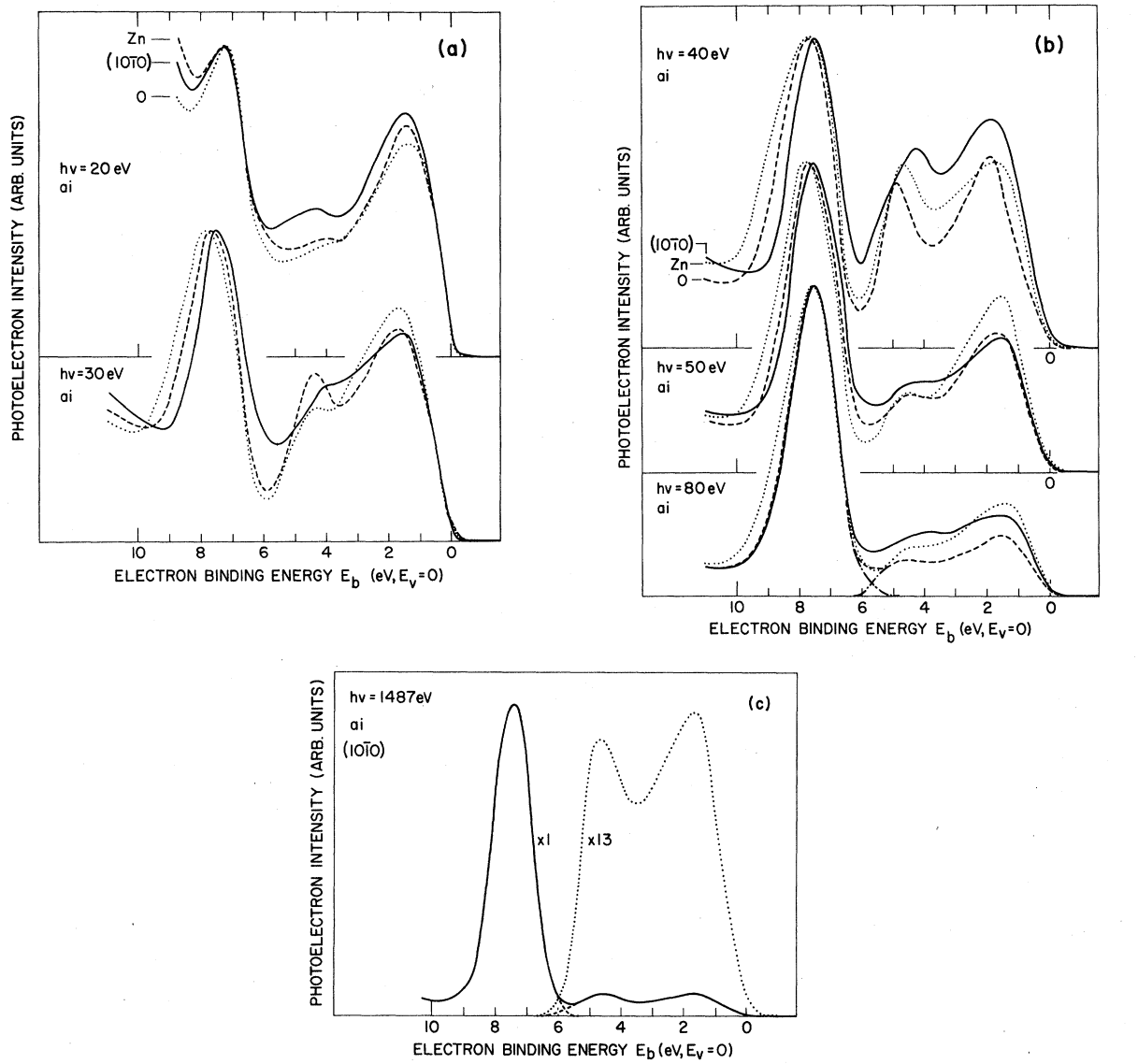

FIG. 2. Angle-integrated (ai) photoelectron spectra from polar (0001) zinc (Zn), polar (000$\bar{1}$) oxygen (O), and nonpolar (10$\bar{1}$0) surfaces of zinc oxide. Zero energy corresponds to the valence-band edge E_v. Spectra are normalized to the the maximum of Zn 3d emission (near 8 eV). (a) Primary photon energies $h\nu = 20$ and 30 eV, (b) $h\nu = 40$, 50, and 80 eV, and (c) $h\nu = 1487$ eV from an Al $K\alpha$ source.

surface atom relaxations on the $(10\bar{1}0)$ surface from photoemission.

A. Angle integrated spectra

Typical results are shown in Fig. 2. The valence band is basically determined by O $2p$ states near $E_b=2$ eV, by Zn $4s-$O $2p$ mixed states near $E_b=4-5$ eV and by Zn $3d$ states near $E_b=7.5$ eV. In no case could intrinsic states be observed in the band gap. This result is in agreement with earlier experimental[11] and theoretical[14] studies.

Valence-band features are less pronounced than observed for the zinc-blende-type semiconductor ZnSe.[1] This finding cannot be explained by differences in the Phillips ionicities of the materials since they are comparable for both compounds with values $f_i=0.616$ (ZnO) and $f_i=0.630$ (ZnSe) (see *Note added in proof*). The physical explanation for this significant difference is the rather different contribution of cation-anion mixed states to the valence-band structure of both II-VI compounds. The anion and cation term values are clearly separated in energy for ZnO with the Zn $4s$ level lying $+7$ eV higher in energy than the O $2p$ level. In consequence, there is only a small Zn $4s$ admixture in the valence bands of ZnO. In particular, the upper part of these bands (from 0 to 3 eV below E_v) is purely O $2p$ derived (see Ref. 14). On the other hand, the anion and cation term values in ZnSe are much closer in energy with the Zn $4s$ level lying even -1 eV below the Se $4p$ on-site energy. A strong mixing of anion and cation states occurs, therefore, in the valence bands of ZnSe giving rise to more directed bonding, stronger dispersion, and sharper valence-band features than in ZnO. Creation of a ZnSe surface thus necessitates the disruption of anion-cation mixed bonding orbitals giving rise to new surface-induced features in the AIPES spectra. This is not the case for ZnO, where ion-derived features dominate the chemical bonding.

All binding energies E_b are referred to the maximum of the valence band E_v. After cleavage, the different surfaces showed different values E_v relative to the vacuum level E_{vac}: $E_{\text{vac}}-E_v=7.9$, 7.6, and 7.4 eV were observed for the nonpolar, Zn, and O surfaces. The differences result from surface-dependent band bending $\Delta(eV_s)$ after cleavage, which had been observed in earlier work-function studies too.[16] It is most probably due to small concentrations (less than 1/100 monolayer) of donor- and acceptor-type lattice imperfections at the surface and can be calculated from $E_{\text{vac}}-E_v$ by taking into account the band-gap energy of 3.2 eV and Fermi energy E_F with $E_F-E_v=3.0$ eV in the bulk at 300 K. Since the Debye screening length of our samples is on the order of 10^{-7} m, which is large compared to the photoelectron escape depth,[17] the spectra are not influenced by the spatial variation of band energies resulting from band bending.

The different surfaces show significantly different photoemission features between $h\nu=30$ and 40 eV which evidently is the range of photon energies yielding maximum surface sensitivity. The separation of emission from surface and bulk electronic states is not straightforward since cross sections for emission from Zn $3d$ near $E_b=7.5$ eV, from Zn $4s-$O $2p$ mixed states near $E_b=4$ eV and from O $2p$ derived states near $E_b=2$ eV show different dependences on photon energies. This can, e.g., be deduced from the variation of relative peak heights with $h\nu$ in Figs. 2(a)–2(c). As a result, surface electronic states cannot be determined by simply subtracting surface-sensitive spectra around $h\nu=35$ eV from bulk spectra at high photon energies even if final-state effects are neglected.

We, therefore, determined the excess emission due to surface states and resonances by subtracting spectra (normalized to the Zn $3d$ peak) with relatively small differences in photon energies but pronounced differences in bulk to surface contributions from each other. Both conditions are, e.g., fulfilled, for difference spectra taken between the $h\nu=40$ and $h\nu=50$ eV spectra [compare Fig. 2(b)]. The standardization to the same Zn $3d$ emission was made, since these states to first approximation do not contribute to the oxygen valence-band features. With the exception of a recent study,[18] any influence of Zn $3d$ on Zn $4s-$O $2p$ and O $2s$ states has been neglected so far in theoretical calculations as well (compare Ref. 14 and references given therein). We separated the Zn $3d$ contribution from the total emission in the valence-band range as indicated by dash-dotted lines in Fig. 2(b) by assuming a Lorentzian decay of the low-energy part of the Zn $3d$ peak. This procedure leads to small systematic errors particularly in the valence-band range of $(10\bar{1}0)$ surfaces above $E_b=5$ eV which will be discussed in a future paper in connection with binding-energy shifts of Zn $3d$ surface states as compared to the bulk binding energy.[19]

In the determination of surface-induced electron emission from photoemission difference spectra, we averaged several difference spectra in order to reduce the influence of final-state effects. The re-

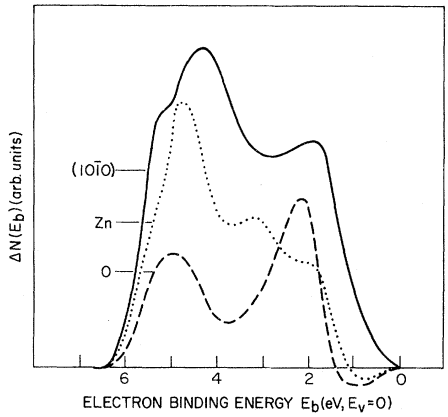

FIG. 3. Photoelectron difference spectra $\Delta N(E_b)$ attributed to emission from surface states and resonances at the different ZnO surfaces. For the determination of $\Delta N(E_b)$ from angle-integrated photoemission spectra taken at different photon energies, see text.

sults shown in Fig. 3 were obtained by averaging the four difference spectra obtained from experiments at $h\nu=50$ and 40 eV, 50 and 30 eV, 60 and 30 eV, and 60 and 40 eV, respectively.

For an identification of these surface features the difference curves in Fig. 3 may be compared with recent theoretical results by Ivanov and Pollmann[14] who determined the integrated layer densities of states (LDOS's) shown in Fig. 4. The peaks near 2 and 5 eV in the difference spectrum of the (10$\bar{1}$0) surface are attributed to the O $2p$ dangling-bond states (P) and to the Zn $4s-$O $2p$ mixed backbond states (B), respectively. The former have their dominant contributions on the surface layer while the latter originate from both the surface and the first subsurface layer [see Fig. 4(a)]. The experimental determination of energetic position and symmetry of the backbond feature B allows for an estimate of the surface atom relaxation at ZnO(10$\bar{1}$0) as will be pointed out in Sec. III B. The polar oxygen surface only gives rise to a pronounced maximum due to O $2p$ dangling-bond states P, whereas the backbond states fill the minimum between 2 eV and about 5 eV on the polar zinc surface. These features compare very well with the theoretical results in Figs. 4(b) and 4(c). Experiment as well as theory also indicates a reduced surface density of states for both polar surfaces at low binding energies $E_b \lesssim 1.2$ eV.

Our evaluation scheme to obtain the $\Delta N(E_b)$ results shown in Fig. 3 over-emphasizes contribu-

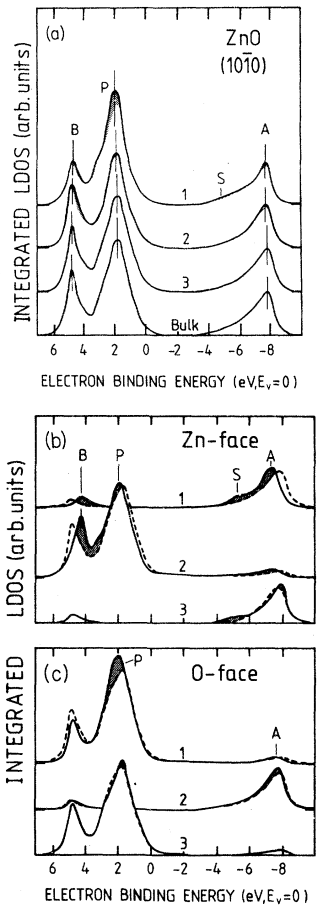

FIG. 4. Theoretical wave-vector-integrated local densities of states (LDOS's) on (a) the first three layers of the relaxed (10$\bar{1}$0) surface, (b) the Zn-terminated, and (c) the O-terminated ZnO surfaces. In (b) and (c) the bulk LDOS is given by dashed lines. Surface-induced positive changes in the LDOS are hatched. Spectra are 0.3-eV Lorentzian broadened. From Ref. 14.

tions above $E_b \approx 3$ eV since the upper part of the valence band is basically O $2p$ derived whereas the lower part with $E_b \gtrsim 3$ eV also contains Zn $4s$ contributions which have significantly increasing cross sections with decreasing photon energies.

B. Angle-resolved spectra

Typical results for normal emission, i.e., Γ in the surface Brillouin zone, are shown in Fig. 5. As found for angle-integrated spectra, significant surface-sensitive features are observed between $h\nu=30$ and 40 eV. At Γ the backbond emission near $E_b=4.5$ eV leads to a pronounced peak on Zn surfaces, is less pronounced on (10$\bar{1}$0), and hard to

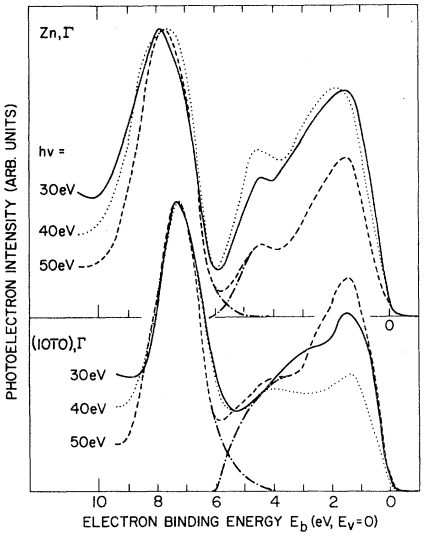

FIG. 5. Angle-resolved photoelectron spectra from the polar (0001) zinc and the nonpolar (10$\bar{1}$0) surface taken at the Γ point with different primary energies $h\nu$.

detect on O surfaces (not shown in the figure), whereas the O $2p$-derived dangling-bond states near $E_b = 2$ eV are pronounced on O surfaces, less pronounced on (10$\bar{1}$0), and hard to detect on Zn surfaces. These results are in line with calculated angle-resolved layer densities of states for ideal ZnO surfaces (see Ref. 14) and thus indicate the existence of geometric structures of polar and nonpolar surfaces as shown in Fig. 1 without significant surface-atom reconstruction or charge transfer between surface and subsurface atoms. The latter may also be deduced from the suprisingly small energetic shifts ΔE_b in the Zn $3d$ binding energy at the surface as compared to the bulk: We determine $\Delta E_b = 0$, $+0.10$, and $+0.18$ eV for the nonpolar (10$\bar{1}$0) and the polar O and Zn surfaces, respectively, from the photon-energy-dependent Zn $3d$ emission.[19]

The ARPES results on (10$\bar{1}$0) will now be discussed in more detail since the theoretical study of relaxation-induced shifts of surface features[14] indicates a strong dependence of the energetic position of backbond states on the geometric position of Zn and O surface atoms. Owing to this geometry-sensitivity of the backbond states B we can derive information about the surface-atom reconstruction from our photoemission results. For this purpose we determined angle-resolved difference spectra $\Delta N(E_b, \vec{k}_{||})$ by means of the same procedure as described in Sec. III A for angle-integrated spectra. Results for the Γ, M, and X points in the surface Brillouin zone are shown in Fig. 6. As expected from the projected band structure the valence-band

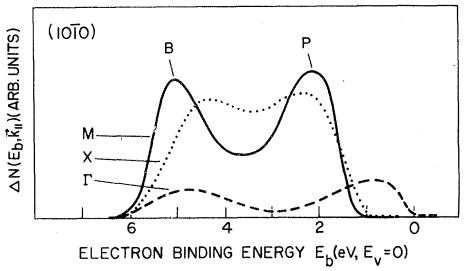

FIG. 6. Photoelectron difference spectra attributed to emission from surface states and resonances at different points in the surface Brillouin zone of the (10$\bar{1}$0) surface. For the determination of $\Delta N(E_b, \vec{k}_{||})$ from angle-resolved photoemission spectra taken at different photon energies, see text.

edge E_v shows significant dispersion. We determine $E_{vac} - E_v = 7.9$, 9.0, and 9.2 eV at Γ, X, and M. The excess emission from surface states or resonances can be analyzed and identified when compared with the theoretical results in Fig. 7. We note that the three difference spectra all consist of double-peak structures. The low binding-energy peaks stem from O $2p$ surface states while the high binding-energy peaks (near 5 eV) originate from the Zn $4s$ – O $2p$ backbonds B. Emission from dangling-bond states P is most pronounced at M and X and is small at Γ. This result correlates nicely with the wave-vector dependence of the surface-layer density of states (shown in Fig. 8 of Ref. 14). The large "pocket" in the projected bulk

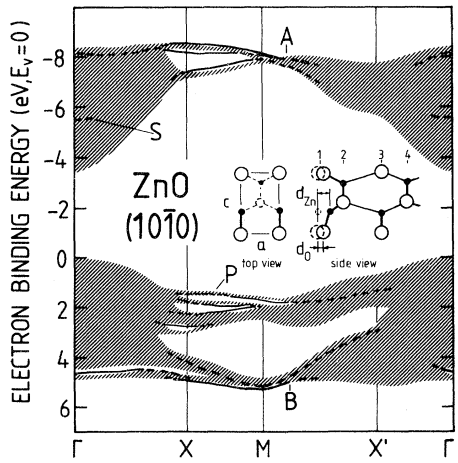

FIG. 7. Surface band structure and projected bulk band structure for the relaxed (10$\bar{1}$0) surface. Bound surface states and pronounced resonances are shown by full lines and dashed lines, respectively. The insets show a top and a side view of the relaxation geometry which was proposed in Ref. 13. From Ref. 14.

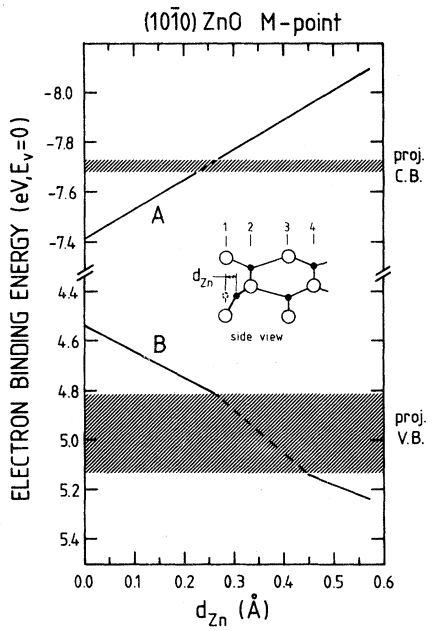

FIG. 8. Relaxation-induced shifts of the covalent surface states A and B at the M point of ZnO(10$\bar{1}$0) as a function of the vertical downward shift d_{Zn} of the top-layer Zn atoms. The O atoms have been held fixed in their unrelaxed positions. The shaded "bands" represent the projected bulk valence and conduction bands at the M point. The inset shows a side view of the studied geometry.

band structure from 2 to 4 eV gives rise to the minimum between the two peaks at X and M.

Finally, we want to use our experimental difference spectrum at M to derive information about surface relaxation of ZnO(10$\bar{1}$0). The experimental difference spectrum at M shows the B maximum at 5.05 eV. Our theoretical investigation of the geometry dependence of surface states at ZnO(10$\bar{1}$0) has shown[14] that the ionic resonances (P,S) are only marginally affected while the covalent surface states (B,A) scale almost linearly with movement of surface-layer Zn atoms towards the bulk. This is shown in Fig. 8. A maximum of backbond state emission (B) at the M point at $E_b = 5.05$ eV is expected from Fig. 8 for a relaxation of Zn atoms by $d_{Zn} = 0.4 \times 10^{-10}$ m.

Within the uncertainty of their determination ($\pm 0.05 \times 10^{-10}$ m), this result on the surface atom displacements is in agreement with results from an earlier dynamical LEED calculation[13] and confirms the proposed structure model for relaxation on ZnO (10$\bar{1}$0) surface by a completely independent method of determination.

Note added in proof. In contrast to ionicity differences f_i on the Phillips scale, corresponding values on the Pauling scale for ZnO ($f_i = 0.795$) and ZnSe ($f_i = 0.575$) explain the general trend towards broadened valence-band features with increasing f_i: The latter scale leads to a better empirical description of bulk bonds with different cation (s)—anion (p) state admixtures to the valence band.

ACKNOWLEDGMENTS

The able assistance of K. Horn and A. Zartner and the staff of the Synchrotron Radiation Center at the University of Wisconsin—Madison is acknowledged. The work was supported by AFOSR under Contract No. F-49620-81-C0089. We thank Professor G. Heiland for supplying us with ZnO single-crystal samples. Two of us (I. I. and J. P.) acknowledge financial support by the Deutsche Forschungsgemeinschaft.

[1]A. Ebina, T. Unno, Y. Suda, H. Koinuma, and T. Takahashi, J. Vac. Sci. Technol. 19, 301 (1981).
[2]R. A. Powell, W. E. Spicer, and J. C. McMenamin, Phys. Rev. Lett. 27, 97 (1971).
[3]R. A. Powell, W. E. Spicer, and J. C. McMenamin, Phys. Rev. B 6, 3056 (1972).
[4]C. J. Veseley, R. L. Hengehold, and D. W. Langer, Phys. Rev. B 5, 2296 (1972).
[5]L. Ley, R. A. Pollak, F. R. McFeely, S. P. Kowalczyk, and D. A. Shirley, Phys. Rev. B 9, 600 (1974).
[6]D. E. Eastman and W. D. Grobman, Solid State Commun. 18, 1427 (1976).
[7]H. Lüth, G. W. Rubloff, and W. D. Grobman, Solid State Commun. 18, 1427 (1976).
[8]W. Ranke, Solid State Commun. 19, 685 (1976).
[9]R. A. Powell and W. E. Spicer, J. Appl. Phys. 48, 4311 (1977).
[10]A. Ebina, K. Asano, Y. Suda, and T. Takahashi, J. Vac. Sci. Technol. 17, 1074 (1980).
[11]W. Göpel, R. S. Bauer, and G. V. Hansson, Surf. Sci. 99, 138 (1980).
[12]W. Göpel, Adv. Solid State Phys. 20, 177 (1980).
[13]C. B. Duke, A. R. Lubinsky, S. C. Chang, B. W. Lee, and P. Mark, Phys. Rev. B 15, 4865 (1977); C. B. Duke, R. J. Meyer, A. Paton, and P. Mark, *ibid.* 18, 4225 (1978).
[14]I. Ivanov and J. Pollmann, Solid State Commun. 36, 361 (1980); J. Vac. Sci. Technol. 19, 344 (1981); Phys. Rev. B 24, 7575 (1981).
[15]D. E. Eastman, J. J. Donelon, N. C. Hien, and F. J.

Himpsel, Nucl. Instrum. Methods 172, 327 (1980).
[16]M. Moormann, D. Kohl, and G. Heiland, Ned. Tijdschr. Vac. Tech. 2, 198 (1979); Surf. Sci. 80, 261 (1979).
[17]W. Göpel and U. Lampe, Phys. Rev. B 22, 6447 (1980).
[18]D. H. Lee and J. D. Joannopoulos, Phys. Rev. B 24, 6899 (1981). The authors show that Zn 3*d* states admix only very little to the higher valence and conduction bands.
[19]W. Göpel and D. E. Eastman, Surf. Sci. Lett. (in press).